Assessing long-term hydrological dynamics and water quality using Google Earth Engine: A case study of Ilgın Lake (1985-2024)

Omer Faruk Atiz[1], Savas Durduran[1]

[1] Necmettin Erbakan University, Geomatics Engineering Dept., Konya, Türkiye - oatiz@erbakan.edu.tr, durduran2001@gmail.com

Keywords: Climate Change, Ecosystem Vulnerability, Google Earth Engine, Lake Water Quality, Shallow Lakes.

Abstract

Monitoring inland water areas is crucial for ecosystem health and water resources management, particularly under impacts of global climate change. Recent advancements in cloud-based platforms like Google Earth Engine (GEE) enable efficient, scalable remote sensing analyses and democratize access to a wide range of data sources. This study leverages the GEE Python API and free and open-source Python libraries (e.g., geemap, scipy, pymannkendall, pingouin) to present a scalable workflow for assessing hydrological and water quality dynamics in shallow lakes. The methodology is demonstrated through a 40-year (1985-2024) case study of Ilgın Lake in Central Anatolia, Türkiye. Based on Landsat 5, 7 and 8 satellite imagery annual water areas, chlorophyll content and turbidity extracted with spectral indices. The climate variables (mean temperature and total precipitation) were extracted from ERA5 (ECMWF Reanalysis Fifth Generation) dataset. The non-parametric Mann-Kendall and Theil Sen's method was used to investigate trends. The relationship between climate factors and water area/water quality were assessed using Pearson correlation, partial correlation analysis and multiple linear regression. Results revealed Ilgın Lake's water area significantly declined, and chlorophyll content significantly increased. All code and workflow are publicly available as Jupyter Notebook on GitHub under the open-source MIT license (`https://github.com/earth-obs/lake-gee-hydrology-water-quality`).

1. Introduction

Inland water bodies are keystone components of ecosystems, particularly in arid and semi-arid regions where agricultural livelihoods largely depend on these water resources. Therefore, precise monitoring of these water sources is indispensable to mitigate the impacts of global climate change, ensure food security, preserve drinking water, and biodiversity (Bogardi et al., 2012).

The European Union Water Framework Directive (WFD) necessitates member states to monitor all water bodies in terms of both water quantity and quality to restore good ecological status (EU, 2000). To comply with the EU Water Framework Directive (WFD), Türkiye's General Directorate of Water Management has initiated the preparation of River Basin Management (RBM) plans for all 25 river basins (Yıldırımer and Demirci, 2024). In Turkey, the legal basis for preparing basin management plans was established in 2012 with the "Regulation on the Preparation, Implementation, and Monitoring of Basin Management Plans" (Ministry of Environment and Urban Planning, Republic of Turkey, 2012).

Continuous monitoring of water levels and water quality parameters requires regular in-situ measurements or IoT-based tracking systems (Hong et al., 2021, Liu et al., 2017). Thus, traditional water management plans prioritize large water bodies due to the labor-intensive nature of data collection and analysis. Remote sensing addresses these challenges by linking spectral reflectance characteristics of water areas to multi-spectral satellite imagery. Initial studies have focused on the extracting of water bodies from land by analyzing spectral differences between water and non-water pixels (McFeeters, 1996, Xu, 2006). Then, remote sensing has been found to be a reliable tool for tracking water quality parameters such as turbidity (Lacaux et al., 2007), chlorophyll concentrations (Mishra and Mishra, 2012) or Secchi disk depth estimations (Lee et al., 2016). Although the remote sensing method is a proof-of-concept for monitoring water resources, it requires expertise in the field to conduct such analyses. For long-term evaluations, a large number of satellite imagery needs to be processed which may also require high-performance hardware.

Recent advancements in cloud-based platforms like Google Earth Engine (GEE) enable efficient, scalable remote sensing analyses and democratize access to a wide range of data sources (Gorelick et al., 2017). There are several studies on the monitoring of water resources using GEE for both water area (Atiz et al., 2023, Li et al., 2024, Lu and Sun, 2023, Owusu et al., 2022, Yilmaz, 2023) and water quality (Das et al., 2024, Dewantoro et al., 2024, Kislik et al., 2022, Tanner et al., 2022, Yan et al., 2025).

While some studies have examined long-term water trends, most primarily focus on either water quantity or water quality. Even in studies that analyze both parameters, the temporal scope is often limited to recent years, neglecting long-term trends essential for understanding climate change impacts. Therefore, this study aims to present a scalable workflow for assessing long-term hydrological dynamics and water quality (1985-2024), leveraging the power of cloud-based GEE and open-source Python libraries, examining this through a case study conducted in Ilgın lake, located in Republic of Türkiye.

2. Data and Methods

2.1 Study Area

Ilgın Lake, also known as Çavuşcu Lake, is a tectonic freshwater lake in Central Anatolia, Türkiye. It has an area of about 2700 hectares, and mean depth is 2-10 m. The lake consists of a small part and a main body, with a dam constructed between them to manage water use for irrigation in the Ilgın district of

Konya. According to Köppen-Geiger climate classification system, the climate of Ilgın is Csa (warm-temperate), characterized by mild winters, and very hot, dry summers (Kottek et al., 2006). Agricultural activities around the lake exert significant anthropogenic pressure on water quality, leading to its classification as a nitrate vulnerable zone under the WFD (T.C. Ministry of Agriculture and Forestry, General Directorate of Water Management, 2023). The lake also serves as a critical habitat for migratory birds and has been designated as a Grade 1 Natural Protected Area in 1992.

2.2 Data

The annual lake area and water quality from 1985 to 2024 were analyzed using satellite images of Landsat-5 TM (Thematic Mapper), Landsat-7 ETM+ (Enhanced Thematic Mapper Plus), and Landsat-8 OLI (Operational Land Imager). However, to ensure temporal continuity, Landsat-5 TM was used until 2011, Landsat-7 ETM+ was employed for 2012, and Landsat-8 OLI was utilized from 2013 to 2024. A summary of the related specifications of Landsat 5, 7 and 8 bands employed in this study, are presented in the Table 1:

Satellite	Bands	Wavelength (µm)
Landsat-5 TM (1985-2011)	B1 – Blue	0.45-0.52
	B2 – Green	0.52-0.60
	B3 – Red	0.63-0.69
Landsat-7 ETM+ (2012)	B4 – NIR	0.76-0.90*
	B5 – SWIR1	1.55-1.75
	B2 – Blue	0.45-0.51
Landsat-8 OLI (2013-2024)	B3 – Green	0.53-0.59
	B4 – Red	0.64-0.67
	B5 – NIR	0.85-0.88
	B6 – SWIR1	1.57-1.65

*For Landsat-7 ETM+ B4: 0.77-90 µm
NIR: Near Infrared
SWIR1: Shortwave Infrared

Table 1. The specifications of the Landsat 5, 7 and 8 bands.

The Landsat images were retrieved using GEE Python API from Collection 2, Tier 1 TOA (top-of-atmosphere) collections, which are recognized as consistent quality and inter-calibrated across sensors (Crawford et al., 2023). First, separate Landsat TOA collections were created by filtering Worldwide Reference System (WRS) path/row coordinates of study area, and maximum of 20% cloudy pixels. After, cloud, cloud shadow and snowy pixels were masked using quality assurance (QA) bands. The data gaps due to the scan line corrector (SLC) failure of Landsat-7 ETM+ were filled using focal_mean() and blend() image functions within GEE. Following, three collections merged into a single image collection, resulting in a total of 347 satellite images from 1984 to 2024, and the annual median composites were derived.

The climate data spanning 1985-2024 were acquired from ERA5 (ECMWF Reanalysis Fifth Generation) using GEE. The ERA5-Land monthly aggregated dataset was selected due to its enhanced spatial resolution, approximately 11 km. The climate parameters included total precipitation sum (Prec) and mean air temperature above 2 m (Temp) across the study area. Monthly precipitation data were aggregated into annual totals in mm, and mean air temperature data were averaged to annual periods in °C.

2.3 Methods

2.3.1 Spectral Indices: The spectral indices were calculated for annual composite images to evaluate water area and water quality variations. The surface waters are sensitive to green band; hence the Modified Normalized Difference Water Index (MNDWI) was utilized to derive lake water area (Xu, 2006). The MNDWI is calculated as follows:

$$MNDWI = \frac{\rho_{Green} - \rho_{SWIR1}}{\rho_{Green} + \rho_{SWIR1}} \tag{1}$$

To distinguish between water and non-water pixels, a suitable threshold value must be selected. The dynamic Otsu thresholds were applied to annual MNWDI images (Otsu et al., 1975), thereby ensuring maximum between-class variance. Subsequently, the MNDWI pixels were classified as water and non-water. The accuracy of water surface extraction was tested using high-quality Google Earth images.

Remote sensing offers several methods to retrieve water quality parameters such as total suspended matter (TSM), chlorophyll-a concentration (Chl-a) and colored dissolved organic matter (CDOM) using remote sensing imagery. These methods mainly rely on empirical or semi-empirical relationships between in-situ observations and spectral reflectance of water pixels (Niroumand-Jadidi et al., 2019).

The Normalized Difference Chlorophyll Index (NDCI) (Mishra and Mishra, 2012) and Normalized Difference Turbidity Index (NDTI) (Lacaux et al., 2007) have been extensively validated for water quality monitoring (Das et al., 2024, Kislik et al., 2022, Mazhar et al., 2023, Singh et al., 2024). Although the NDCI was originally developed for MERIS (Medium Resolution Imaging Spectrometer) using 708 nm and 665 nm spectral bands, it has been successfully adapted to Landsat-8 OLI by substituting closest available NIR and Red bands (Buma and Lee, 2020). In this study, we similarly utilized NIR and Red bands for Landsat-5 TM, Landsat-7 ETM+ to ensure consistency across the Landsat series. Water quality within water-masked areas was assessed using NDCI for chlorophyll concentration and the NDTI for turbidity leveraging Landsat-5 TM, Landsat-7 ETM+ and Landsat-8 OLI imagery. These indices are formulated as follows:

$$NDCI = \frac{\rho_{NIR} - \rho_{Red}}{\rho_{NIR} + \rho_{Red}} \tag{2}$$

$$NDTI = \frac{\rho_{Red} - \rho_{Green}}{\rho_{Red} + \rho_{Green}} \tag{3}$$

While this approach provides a scalable solution for water area extraction and water quality assessment without requiring in-situ calibration, its performance may vary across water bodies due to site-specific variations in hydrological, biological and optical properties (Das et al., 2024, Lopez, 2023).

2.3.2 Trend Analysis: Long-term trends in water area, water quality and climate variables were analyzed using the non-parametric Mann-Kendall test (Mann, 1945) and Theil-Sen slope methods (Sen, 1968, Theil, 1992). The Mann-Kendall test evaluates the statistical significance of monotonic trends, while the Theil-Sen slope quantifies the magnitude of trends, providing robustness against outliers and non-normal data distributions. This approach ensures reliable detection of trends in environmental time series.

2.3.3 Correlation and Multiple Linear Regression Analysis: Relationships between variables (water area, Prec, Temp, NDCI, NDTI) were assessed using Pearson's correlation coefficients. In addition, partial correlations were computed to isolate the effects of precipitation and temperature on water area while controlling for confounding variables. A multiple linear regression (MLR) model was developed to quantify the combined influence of temperature and precipitation on annual water area variations. The MLR equation is expressed as:

$$Water\ Area = \beta_0 + \beta_1 \times Temp + \beta_2 \times Prec + \epsilon \quad (4)$$

where β_0 is the intercept, β_1 and β_2 are regression coefficients, and ϵ represents the error term. In addition, 1-year lagged effect of $Prec$ is also examined by substituting $Prec$ with $Prec_{lag-1}$.

3. Results and Discussions

The accuracy of annual water area extraction was assessed using high-resolution Google Earth image at 05.10.2010 and Landsat-5 TM image at 26.09.2010 using 250 random sample points. A confusion matrix was generated based on random sample points, and overall accuracy of 96.0% and Kappa coefficient of 0.887 were computed. Therefore, the accuracy of water area extraction method was found reliable. Furthermore, the inter-annual variations of the Otsu threshold are presented in Figure 1. The dynamic Otsu threshold values were ranged between 0.14 and 0.29, which indicates the spectral reflectance of water pixels are not stable over time. The reason for this may be related to differing water quality conditions.

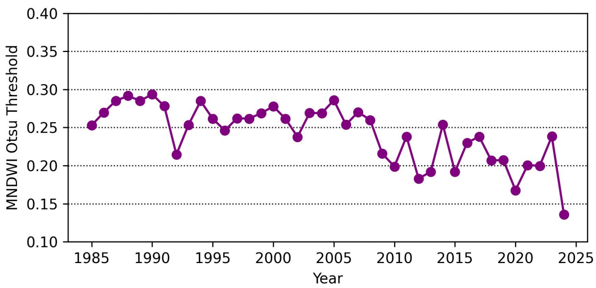

Figure 1. The inter-annual Otsu threshold.

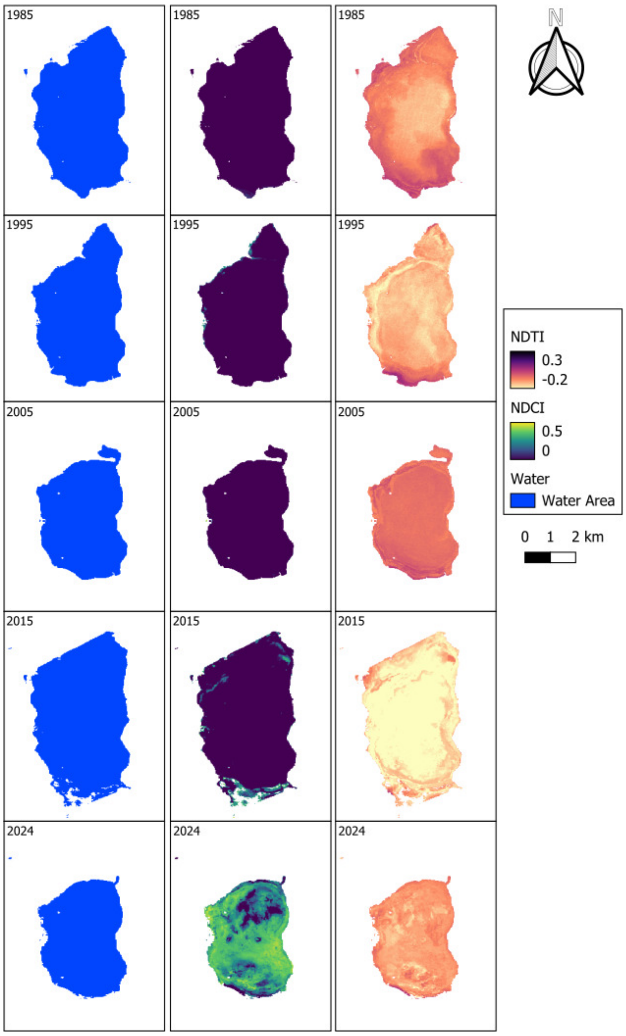

Figure 2. Lake water area, NDCI, and NDTI at 10 year intervals.

The water surface area, NDCI, and NDTI at 10 year interval are shown in Figure 2. A broad overview of the lake's transformation over decadal intervals (1985, 1995, 2005, 2015, and 2024) shows a clear trend of diminishing surface area alongside steadily rising chlorophyll concentrations. These patterns are reflected in the Normalized Difference Chlorophyll Index (NDCI) and the Normalized Difference Turbidity Index (NDTI), both of which were evaluated at annual time period to capture the lake's ecological status.

The interpretation of NDCI and NDTI values is as follows (Rawat et al., 2023):

- NDCI < 0.0 indicates very low,
- $0.0 - 0.2$ indicates low,
- $0.2 - 0.5$ indicates moderate,
- NDCI > 0.5 indicates high chlorophyll content.

For turbidity (NDTI):

- NDTI < 0.05 indicates low turbidity,
- $0.05 - 0.2$ indicates moderate turbidity,
- NDTI > 0.2 indicates high turbidity.

In the following analyses, NDCI and NDTI values below zero are excluded. The annual variations of water surface area, NDCI, and NDTI between 1985 and 2024 are illustrated in Figure 3.

The water area patterns between 1985 and 2015 exhibit year-to-year variations, with a notable decline in the last decade. The overall average water area of Ilgın Lake is 1997.8 ha, with a maximum of 2627.8 ha recorded in 1996 and a minimum of 1434.2 ha in 2018. While turbidity in Ilgın Lake appears relatively stable, chlorophyll concentrations increased remarkably in certain years (1998, 2000, 2019, 2021, 2024). In recent years, NDCI values increased above 0.2, indicating moderate chlorophyll concentrations. The maximum NDCI value in

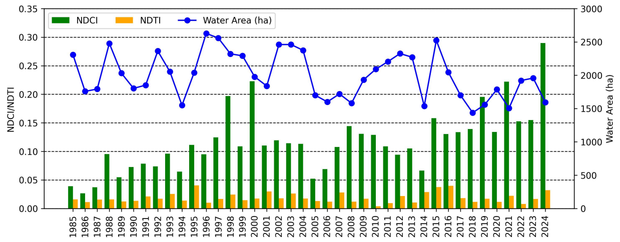

Figure 3. Annual variations of water surface area, NDCI, and NDTI between 1985 and 2024.

2024 suggests that Ilgın Lake's annual eutrophication level is at its highest over the past 40 years. During the relatively stable years from 2010 to 2014, Ilgın Lake exhibited low turbidity and low chlorophyll content. These findings align with a field study conducted in 2010–2011, which classified Ilgın Lake as high-quality based on its physicochemical status and eutrophication level (Aşıkkutlu et al., 2014).

Before further analyzing the results, Figure 4 displays the histograms of key climate and water quality parameters. As seen in Figure 3, the annual total precipitation ranged from 261 to 480 mm, temperatures fluctuated between 8 and 13 °C, NDCI values ranged 0.03 to 0.29, and NDTI values remained consistently low as below 0.04. These ranges indicate the relatively stable turbidity conditions compared to moderate variability in chlorophyll and climate factors.

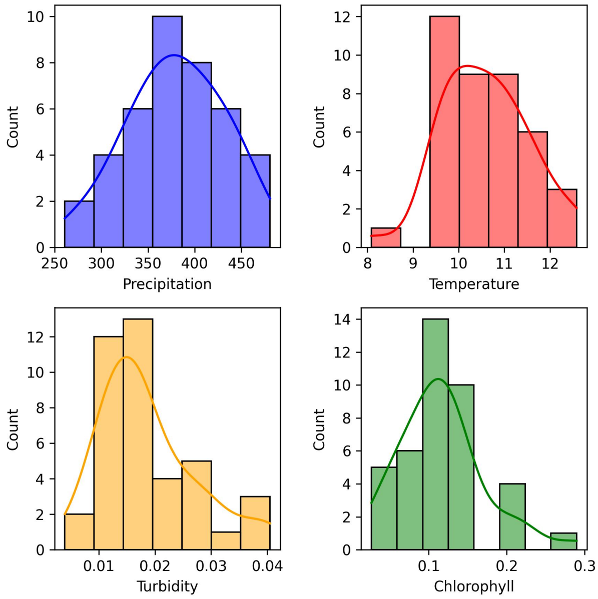

Figure 4. The histograms of climate and water quality parameters.

The Mann-Kendall and Sen Slope's trend results are given in Table 2. The results show a statistically significant reduction in water surface area, estimated at -9.54 hectares per year ($p < 0.05$). This decline corresponds to approximately 31% loss of the lake's extent, suggesting that Ilgın Lake is sensitive to both climatic fluctuations and anthropogenic pressures.

The mean temperature shows a statistically significant positive trend ($p < 0.01$) of 0.05 $^\circ C$ per year, aligning with broader regional warming trends. Total annual precipitation did not exhibit a statistically significant monotonic trend ($p > 0.05$). The water quality parameters underscore important ecological shifts. NDCI shows a significant upward trend ($p < 0.01$), implying increased eutrophication processes, likely tied to nutrient inputs from the surrounding watershed and the influence of warmer temperatures that can accelerate algal growth. This result is in line with local management interventions, such as the recent reed-clearing efforts in Lake Ilgın, aimed at mitigating excessive vegetation growth and controlling the negative impacts of eutrophication (Konhaber, 2020). Recent local news reported severe drought conditions at Ilgın Lake, supporting our findings of ecological stress though reduced water levels and biodiversity losses (Konhaber, 2024). The turbidity did not show a clear monotonic increase or decrease over the study period.

	Trend	Slope	P-Value	Z-Score	Conf.
Area	$-$	**-9.5392**	0.0463	-1.9923	95.4%
Prec	n/a	-0.2121	0.8067	-0.2447	19.3%
Temp	$+$	**0.0528**	0.0000	4.3924	100.0%
Turb	n/a	0.000	0.5840	0.5476	41.6%
Chl-a	$+$	**0.0028**	0.0000	4.7886	100.0%

Note: Bold indicates significant trends
$+, -$:Increasing and decreasing trends

Table 2. Mann-Kendall and Sen Slope's trend results.

Furthermore, Figure 5 illustrates the relationships of key climate variables and water quality parameters on the water area change using scatter plots. A distinct association between temperature and water area was found.

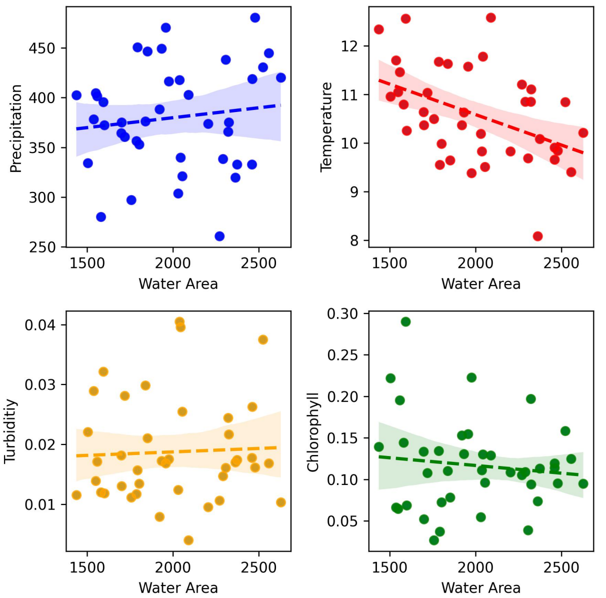

Figure 5. Scatter plots of water area against key climate variables and water quality parameters.

Pearson's correlation analysis was used to see how these variables relate. Table 3 shows the correlation matrix for hydrological and water quality parameters. A moderate negative correlation ($r = -0.4466$) was found between water area and temperature. Temperature was also positively correlated ($r = 0.3958$) with NDCI, indicating that warming increases eutrophication. NDTI also shows a low positive correlation ($r = 0.2671$) with NDCI, suggesting that higher chlorophyll content may associated with turbidity.

	Area	Prec	Temp	Turb	Chl-a
Area	1.0000	0.1309	**-0.4466**	0.0460	-0.1170
Prec	0.1309	1.0000	-0.0402	0.1208	0.0818
Temp	**-0.4466**	-0.0402	1.0000	0.1021	**0.3958**
Turb	0.0460	0.1208	0.1021	1.0000	0.2671
Chl-a	-0.1170	0.0818	**0.3958**	0.2671	1.0000

Note: Bold indicates significant correlations ($p < 0.05$)

Table 3. Pearson's correlation matrix.

On the other hand, annual precipitation shows only a weak correlation with the lake's surface area ($r = 13.09$) when analyzed within the same year. This weak correlation may be due to the complex hydrological dynamics of shallow lakes, where water inputs can vary over different timescales or be influenced by human activities such as irrigation. Additionally, the annual analysis in this study may not fully capture delayed hydrological responses to precipitation, possibly due to seasonal variations. Therefore, the 1-year delayed response of annual total precipitation was included in the correlation and subsequent analysis. This improved the correlation between water area and precipitation to 0.3428 ($p < 0.05$), suggesting a delayed response of precipitation.

Moreover, the partial correlation coefficients (PCCs) between water area, water quality and climate parameters were calculated to isolate individual effects of Prec and Temp. The PCC results are given in Table 4. The PCCs between NDTI and climate variables are not included as they do not show statistically significant correlations. As provided in Table 4, the significant correlation coefficients did not change substantially. However, including 1-year lagged precipitation strengthened the relationship between water area to moderate level ($r = 0.4351$)

Correlation	PCC	P-Value
Area-Temp	**-0.4455**	0.0045
Area-Prec	0.1263	0.4436
Area-Prec$_{lag-1}$	**0.4351**	0.0063
Chl-Temp	**0.4007**	0.0115
Chl-Prec	0.1065	0.5187
Chl-Prec$_{lag-1}$	0.1696	0.3086

Note: Bold indicates significant PCCs ($p < 0.05$)

Table 4. Partial correlation results.

According to the MLR results using same year precipitation data, climate variables explained 21% of annual water area fluctuations ($R^2 = 0.21,\ p < 0.05$). However, substituting same year precipitation with 1-year lagged precipitation ($Prec_{lag-1}$) improved the model's explanatory power to $R^2 = 0.34$ ($p < 0.05$). The final MLR equation with 1-year lagged precipitation is given in Equation 5:

$$Water\ Area = 2823.17 - 170.12 \times Temp + 2.56 \times Prec_{lag-1} \quad (5)$$

This suggests that a 1 °C increase in temperature corresponds to a 170.12 ha decline water area, while 1 mm increase in 1-year lagged precipitation increases water area by 2.56 ha ($p < 0.05$). Despite these statistically significant relationships, the relatively low R^2 value suggests that unaccounted factors such as other climatic or anthropogenic activities likely drive additional variability. For instance, agricultural practices around Ilgın Lake, particularly irrigation and fertilizer use, may play a critical role, as evidenced by its designation as nitrate vulnerable zone. This highlights the Ilgın Lake's sensitivity to nutrient pollution, further supporting the hypothesis that human activities significantly influence water area dynamics.

Although, this study demonstrates the role of long term Landsat imagery for monitoring water resources, the accuracy of used spectral indices such as NDCI and NDTI may vary significantly across water bodies due to differences in biological and optical properties (Das et al., 2024, Lopez, 2023). However, shallow eutrophic lakes like Ilgın Lake are particularly more suitable to the proposed workflow. In addition, different climatic variables from ERA5 dataset may be included for more in-depth analysis on the effect of climate or human activities over water resources.

4. Conclusions

The findings of this study underscore the vulnerability of shallow lakes like Ilgın Lake to ecological degradation, driven by both climatic variations and human activities. Their limited water depth increases risks to sustainable agriculture, biodiversity, and local socio-economic conditions. To address the challenges, we proposed a workflow leveraging cloud-based GEE platform and Python tools, enabling scalable and cost-effective monitoring of water area and water quality dynamics. This approach provides valuable insights into sustainable water resource management plans, especially for regions where in-situ data is unavailable. This study aligns with the EU WFD goals for monitoring water bodies listed under Annex V. The water resource monitoring studies should focus not only on the hydrological context but also on water quality status, as both are essential for holistic water management. Additionally, shallow lakes like Ilgın play a critical role in preserving natural habitats and sustaining local agricultural livelihoods. Future work will extend this framework to higher resolution satellite data (e.g., Sentinel-2) and additional spectral indices to refine estimates of water quality parameters. All code and workflow are publicly available as Jupyter Notebook on GitHub (`https://github.com/earth-obs/lake-gee-hydrology-water-quality`) under the open source MIT license.

References

Atiz, O. F., Alkan, T., Durduran, S., 2023. Google Earth Engine Based Spatio-Temporal Changes of Bafa Lake from 1984 to 2022. *International Journal of Environment and Geoinformatics*, 10(3), 116–123.

Aşıkkutlu, B., Akköz, C., Öztürk, B. Y., 2014. Some Water Quality Characteristics of Çavuşçu Lake (Konya/Ilgın). *Selçuk University Faculty of Science Journal*, 39, 1–9.

Bogardi, J. J., Dudgeon, D., Lawford, R., Flinkerbusch, E., Meyn, A., Pahl-Wostl, C., Vielhauer, K., Vörösmarty, C., 2012. Water security for a planet under pressure: interconnected challenges of a changing world call for sustainable solutions. *Current Opinion in Environmental Sustainability*, 4(1), 35-43. Open issue.

Buma, W. G., Lee, S.-I., 2020. Evaluation of sentinel-2 and landsat 8 images for estimating chlorophyll-a concentrations in lake Chad, Africa. *Remote Sensing*, 12(15), 2437.

Crawford, C. J., Roy, D. P., Arab, S., Barnes, C., Vermote, E., Hulley, G., Gerace, A., Choate, M., Engebretson, C., Micijevic,

E. et al., 2023. The 50-year Landsat collection 2 archive. *Science of Remote Sensing*, 8, 100103.

Das, S., Nandi, D., Thakur, R. R., Bera, D. K., Behera, D., Ðurin, B., Cetl, V., 2024. A Novel Approach for Ex Situ Water Quality Monitoring Using the Google Earth Engine and Spectral Indices in Chilika Lake, Odisha, India. *ISPRS International Journal of Geo-Information*, 13(11), 381.

Dewantoro, M., Ulfa, M., Supatmanto, B., 2024. Water turbidity mapping using sentinel-2a imagery and cloud based google earth engine in saguling reservoir. *IOP Conference Series: Earth and Environmental Science*, 1343, IOP Publishing, 012027.

EU, 2000. Directive 2000/60/EC of the European Parliament and of the Council of 23 October 2000 establishing a framework for Community action in the field of water policy. *Official Journal of the European Communities*, 327(43), 1–72.

Gorelick, N., Hancher, M., Dixon, M., Ilyushchenko, S., Thau, D., Moore, R., 2017. Google Earth Engine: Planetary-scale geospatial analysis for everyone. *Remote sensing of Environment*, 202, 18–27.

Hong, W. J., Shamsuddin, N., Abas, E., Apong, R. A., Masri, Z., Suhaimi, H., Gödeke, S. H., Noh, M. N. A., 2021. Water Quality Monitoring with Arduino Based Sensors. *Environments*, 8(1).

Kislik, C., Dronova, I., Grantham, T. E., Kelly, M., 2022. Mapping algal bloom dynamics in small reservoirs using Sentinel-2 imagery in Google Earth Engine. *Ecological Indicators*, 140, 109041.

Konhaber, 2020. Cleaning efforts started at Çavuşcugöl. Accessed: 2024-03-18.

Konhaber, 2024. It was declared a natural protected area 32 years ago: This lake in konya was also hit by drought. Accessed: 2024-03-18.

Kottek, M., Grieser, J., Beck, C., Rudolf, B., Rubel, F., 2006. World Map of the Köppen-Geiger climate classification updated. *Meteorologische Zeitschrift*, 15(3), 259-263. http://dx.doi.org/10.1127/0941-2948/2006/0130.

Lacaux, J., Tourre, Y., Vignolles, C., Ndione, J., Lafaye, M., 2007. Classification of ponds from high-spatial resolution remote sensing: Application to Rift Valley Fever epidemics in Senegal. *Remote sensing of environment*, 106(1), 66–74.

Lee, Z., Shang, S., Qi, L., Yan, J., Lin, G., 2016. A semi-analytical scheme to estimate Secchi-disk depth from Landsat-8 measurements. *Remote sensing of environment*, 177, 101–106.

Li, X., Zhang, F., Shi, J., Chan, N. W., Cai, Y., Cheng, C., An, C., Wang, W., Liu, C., 2024. Analysis of surface water area dynamics and driving forces in the Bosten Lake basin based on GEE and SEM for the period 2000 to 2021. *Environmental Science and Pollution Research*, 31(6), 9333–9346.

Liu, H., Li, Q., Shi, T., Hu, S., Wu, G., Zhou, Q., 2017. Application of Sentinel 2 MSI Images to Retrieve Suspended Particulate Matter Concentrations in Poyang Lake. *Remote Sensing*, 9(7). https://www.mdpi.com/2072-4292/9/7/761.

Lopez, A. G., 2023. Assessing the use of normalized difference chlorophyll index to estimate chlorophyll-a concentrations using landsat 5 tm and landsat 8 oli imagery in the salton sea, california. M.S. thesis, University of Southern California.

Lu, L., Sun, H., 2023. Dynamic monitoring of surface water areas of nine plateau lakes in Yunnan Province using long time-series Landsat imagery based on the Google Earth Engine platform. *Geocarto International*, 38(1), 2253196.

Mann, H. B., 1945. Nonparametric tests against trend. *Econometrica: Journal of the econometric society*, 245–259.

Mazhar, N., Javid, K., Akram, M. A. N., Afzal, A., Hamayon, K., Ahmad, A., 2023. Index-Based Spatiotemporal Assesment Of Water Quality In Tarbela Reservoir, Pakistan (1990- 2020). *Geography, Environment, Sustainability*, 15(4), 232–242.

McFeeters, S. K., 1996. The use of the Normalized Difference Water Index (NDWI) in the delineation of open water features. *International journal of remote sensing*, 17(7), 1425–1432.

Ministry of Environment and Urban Planning, Republic of Turkey, 2012. Regulation on the preparation, implementation, and monitoring of basin management plans. T.C. Official Gazette. Official Gazette Date: 17 October 2012; Official Gazette Issue: 28444.

Mishra, S., Mishra, D. R., 2012. Normalized difference chlorophyll index: A novel model for remote estimation of chlorophyll-a concentration in turbid productive waters. *Remote Sensing of Environment*, 117, 394–406.

Niroumand-Jadidi, M., Bovolo, F., Bruzzone, L., 2019. Novel spectra-derived features for empirical retrieval of water quality parameters: Demonstrations for OLI, MSI, and OLCI Sensors. *IEEE Transactions on Geoscience and Remote Sensing*, 57(12), 10285–10300.

Otsu, N. et al., 1975. A threshold selection method from gray-level histograms. *Automatica*, 11(285-296), 23–27.

Owusu, C., Snigdha, N. J., Martin, M. T., Kalyanapu, A. J., 2022. PyGEE-SWToolbox: A Python Jupyter Notebook Toolbox for Interactive Surface Water Mapping and Analysis Using Google Earth Engine. *Sustainability*, 14(5), 2557.

Rawat, K. S., Sahu, S. R., Singh, S. K., Chander, S., Gujrati, A., 2023. Water quality analysis using normalized difference chlorophyll index (ndci) and normalized difference turbidity index (ndti), using google earth engine platform. *2023 International Conference on Modeling, Simulation & Intelligent Computing (MoSICom)*, 408–413.

Sen, P. K., 1968. Estimates of the regression coefficient based on Kendall's tau. *Journal of the American statistical association*, 63(324), 1379–1389.

Singh, R., Saritha, V., Pande, C. B., 2024. Monitoring of wetland turbidity using multi-temporal Landsat-8 and Landsat-9 satellite imagery in the Bisalpur wetland, Rajasthan, India. *Environmental Research*, 241, 117638.

Tanner, K. B., Cardall, A. C., Williams, G. P., 2022. A spatial long-term trend analysis of estimated chlorophyll-a concentrations in Utah Lake using Earth observation data. *Remote Sensing*, 14(15), 3664.

T.C. Ministry of Agriculture and Forestry, General Directorate of Water Management, 2023. Sakarya basin river basin management plan preparation project: River basin management plan report. Technical report, T.C. Ministry of Agriculture and Forestry, General Directorate of Water Management, Ankara, Türkiye. [Sakarya Havzası Nehir Havza Yönetim Planı Hazırlanması Projesi: Nehir Havza Yönetim Planı Raporu].

Theil, H., 1992. A rank-invariant method of linear and polynomial regression analysis. *Henri Theil's contributions to economics and econometrics: Econometric theory and methodology*, Springer, 345–381.

Xu, H., 2006. Modification of normalised difference water index (NDWI) to enhance open water features in remotely sensed imagery. *International journal of remote sensing*, 27(14), 3025–3033.

Yan, N., Qiu, Z., Zhang, C., Liu, J., Liu, D., 2025. Observing water turbidity in Chinese rivers using Landsat series data over the past 40 years. *Journal of Cleaner Production*, 145001.

Yilmaz, O. S., 2023. Spatiotemporal statistical analysis of water area changes with climatic variables using Google Earth Engine for Lakes Region in Türkiye. *Environmental Monitoring and Assessment*, 195(6), 735.

Yıldırımer, S., Demirci, U., 2024. The reflections of international developments in watershed management approaches on policy and strategy documents in Türkiye. *The Anatolian Journal of Forest Research*, 10(1), 78–90.